Journal of
Manufacturing and Materials Processing

MDPI

Article

Fabrication of Highly Compacted Green Body Using Multi-Sized Al Powder under a Centrifugal Force

Bakytzhan Sariyev [1,*], Abilkhairkhan Aldabergen [1], Dulat Akzhigitov [1], Boris Golman [2,*] and Christos Spitas [1]

[1] Department of Mechanical and Aerospace Engineering, School of Engineering and Digital Sciences, Nazarbayev University, Nur-Sultan 010000, Kazakhstan; abilkhairkhan.aldabergen@alumni.nu.edu.kz (A.A.); dulat.akzhigitov@mail.polimi.it (D.A.); research.spitas@gmail.com (C.S.)
[2] Department of Chemical and Materials Engineering, School of Engineering and Digital Sciences, Nazarbayev University, Nur-Sultan 010000, Kazakhstan
* Correspondence: bakytzhan.sariyev@nu.edu.kz (B.S.); boris.golman@nu.edu.kz (B.G.)

Abstract: This study investigates the application of centrifugal force for the compaction of metal powder. Previous studies using the centrifugal force for manufacturing the green bodies were focused on fine powders with narrow particle size distribution or binary mixtures. This study explores the particle packing of multi-sized powder. Aluminum alloy powder with a particle size less than 100 µm and polymer binder were admixed and compacted in the centrifugal casting with ranging magnitudes of centripetal acceleration. Three different centrifugal forces were tested: 700, 1800, and 3700 *G*. The microstructure of the green bodies was then observed on the SEM micrographs. The obtained green bodies had high packing densities ranging from 62 to 69%. The packing density and median particle size increase at the positions further away from the center of rotation of the centrifuge with an increase of centrifugal force. The effect of centrifugal force on the segregation of particles was investigated through the quasi-binary segregation index. The segregation phenomena was not observed at 700 *G*, but clear particle segregation was found at higher centrifugal forces. The increase of the centrifugal force resulted in higher segregation with finer particles moving to the inner part of the spinning mold, with a significant change in the size of particles located closer to the center of rotation. Overall, the centrifugal process was found to produce highly compacted green bodies while yielding a segregation effect due to wide particle size distribution.

Keywords: compaction; centrifugal force; green body; multi-sized metal powder; segregation

Citation: Sariyev, B.; Aldabergen, A.; Akzhigitov, D.; Golman, B.; Spitas, C. Fabrication of Highly Compacted Green Body Using Multi-Sized Al Powder Under a Centrifugal Force. *J. Manuf. Mater. Process.* **2022**, *6*, 79. https://doi.org/10.3390/jmmp6040079

Academic Editor: Steven Y. Liang

Received: 13 June 2022
Accepted: 11 July 2022
Published: 22 July 2022

1. Introduction

Powder metallurgy (PM) is a growing field of modern-day manufacturing and plays a significant role in the fabrication of high-quality tools and parts. The principal part of PM is the forming process, which is currently an object of substantial research efforts. The majority of the research is dedicated to the improvement of different compaction techniques, the essential purpose of which is to form a green body with a high density and requested mechanical properties [1–3]. The mechanical properties of PM parts are all functions of their porosity [4,5]. The strength of a material, i.e., its elastic modulus, fracture modulus, etc., is inversely dependent on the porosity [6]. Control of void fraction and packing efficiency is, therefore, a vital part of PM [7,8], and is usually done by adjusting the forming pressure and particle size of the powder. Other important factors affecting the mechanical properties of PM parts include the sintering parameter and homogeneity of microstructure [9–12].

All of the above mentioned factors constitute a significant limitation of isostatic compression, a common forming process in PM, and restrict the manufacturing of parts to a few simple shapes [13]. Recently introduced, Centrifugal Compaction Process (CCP) may resolve most of the problems of PM. During CCP, the centrifugal forces due to the centrifugal acceleration, which forms when the cast is rotated around a certain axis, are dominant

compared to other forces exerted on particles. Contrary to pressure casting, where both particles and the medium move in the same direction, the centrifugal force directly applies to the particles in the slip, forcing the particles to move in the direction exerted by that force for compaction and the medium to move in the opposite direction. Consequently, the countercurrent motion of particles and the medium significantly shortens the compaction time [14]. Furthermore, this sedimentation mechanism of CCP leaves the green body without defects such as filtration channels, which are common in slip casting and pressure filtration [15,16]. CCP allows fabricating the green bodies with homogeneous and flawless microstructure, leading to the product having superior sintering ability, higher strength, and hardness [2,17]. The other advantages of the centrifugal method include its economic feasibility [18] and excellent shape transcription from the die [17]. All of this enables to produce large parts with a reduced risk of failure using CCP, which makes it an attractive solution for the manufacturers [15].

Usually, materials with uniform microstructure and pore size distribution are more suitable for engineering applications than those with nonuniform microstructure and wide pore size distribution [19]. In this aspect, CCP is different from other methods as it induces particle segregation due to differential settling of different sized particles, as larger particles experience more significant centrifugal force [20]. However, such a feature of CCP is beneficial for the production of Functionally Graded Materials (FGM), a promising class of materials characterized by spatial variation of material composition [21–25]. Mainly, the arrangement of the powder in FGM is stepwise or continuously graded. In the case of continuous grading, the change in material properties is gradual throughout the material body [26]. Several studies were made on the analysis of segregation and the creation of a compositional gradient body using the centrifugal method [18,27–33]. The results of these works show that the centrifugal force moves larger particles in the mixture to the outer part of the spinning mold, leading to the compaction of particles. Additionally, the increase of centrifugal force was shown to increase the gradient of segregation [27]. The centrifugal force is specified by the G number, which is the ratio of centrifugal force to the gravity:

$$G = \frac{\omega^2 R}{g}, \tag{1}$$

where ω is the mold rotational speed (rad/s), R is the cast ring radius (m), and g is the acceleration due to gravity (m/s^2). It is well known that most of the industrially applied powders are polydisperse or multi-sized, particle mixtures, but the majority of experimental research on particle segregation is focused on binary mixtures [34,35]. Although several studies of compaction and segregation of materials manufactured by the centrifugal method have been previously conducted, the application of CCP using the multi-sized powder for the fabrication of highly compacted green bodies was not explored thoroughly. In the present work, we study the compaction and segregation of multi-sized aluminum alloy powder, which is frequently used in the automotive industry due to its high mechanical properties, heat, and wear resistance. Because of their low density, fine particle size, and irregular shape, aluminum alloy particles possess limited flowability. These factors frequently cause the formation of the loosely packed green body with large pores [36], making the aluminum alloy powder the promising material for the study of the application of CCP. In our study, we used Al powder with a wide particle size distribution from 5 µm to 100 µm. It is a common knowledge that at a greater size ratios, the smaller particles can fit in the interstitial positions of the larger particle packing structure, leading to higher packing density. Therefore, at higher particle size ratio of the mixture, a higher packing density of the green compact can be obtained [37–40].

2. Materials and Methods

This study used commercial CL 30AL Aluminum alloy powder [Concept Laser GmbH. Lichtenfels, Germany] with a wide particle size distribution depicted in Figure 1. The powder was dispersed in the epoxy adhesive with a 40% of solid volume fraction [Ekoklass].

The epoxy adhesive has a density of 1.25 g/cm^3. The prepared premixed slurry was poured into the dies and loaded into the centrifugal machine [Allegra X-14 Beckman Coulter Inc. Brea, CA, USA]. Test tubes with a conical bottom were used as the dies. The die was tilting along the horizontal axis of the centrifugal force.

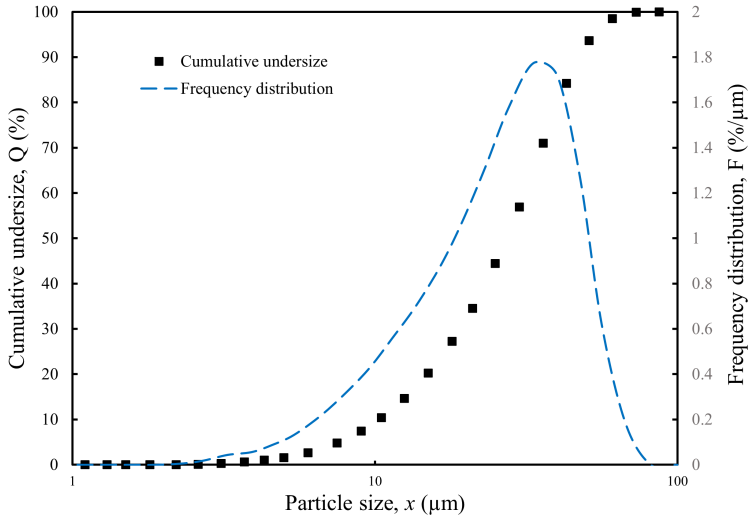

Figure 1. Size distribution of Al alloy powder.

The compaction of the powder was performed at several different *G* values using a centrifugal machine. Three different centrifugal forces, *G*, were considered: 700, 1800, and 3700. The rotational time was set to 180 min to let the specimens fully solidify during the centrifugal acceleration. The temperature was set to 40 °C, which is a recommended temperature for the solidification of epoxy adhesive. The powder from the same batch is used for all experiments. Consequently, the same composition and temperature conditions were used for different values of centrifugal forces. The rotation of slurry in the centrifuge for 180 min results in sedimentation and compaction of powder in the dies under the centrifugal force. After compaction, the fabricated green bodies are removed from the dies. Figure 2 shows the fabricated green body. As it can be seen, the application of the centrifugal force results in clear segregation of Al powder and epoxy adhesive. Aluminum particles having higher density move to the outer region, away from the axis of rotation of the centrifuge in a radial direction, while epoxy adhesive of lower density moves to the inner region. The green body has taken the shape of the die due to excellent shape transcription. Each sample was then sliced for its cross-sectional analysis using a wet abrasive cut-off machine (Brillant 220 QATM. Mammelzen, Germany). After sectioning, samples were polished by graded sandpapers (800, 1200, 2500 grit), and finally by alumina suspensions of 1 µm, 0.3 µm, and 0.05 µm. A scanning electron microscope (JSM-IT200 JEOL Ltd. Tokyo, Japan) was used to examine the microstructure of the fabricated green bodies. It was operated at 15 kV under secondary electron mode. A thin gold coating (5 µm) was applied to the specimens to obtain a conductive surface for further SEM investigations.

To analyze the microstructure and the effect of segregation due to the centrifugal force, the microstructure was observed for 4 different locations varying with radial position from the center of rotation of the centrifuge. Figure 3 illustrates the schematics of the specimen analyzed with SEM. The radial position in the sample was normalized from 0 (inner sample boundary) and 1 (outer sample boundary). The microstructure was observed at radial positions of 0.2, 0.4, 0.6, and 0.8.

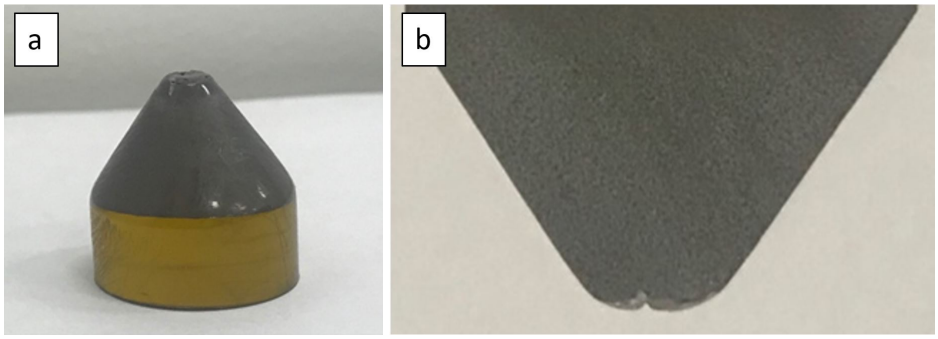

Figure 2. Green body fabricated under centrifugal force of 3700 *G*, (**a**) sample extracted from the die, and (**b**) cross-sectional view of the specimen.

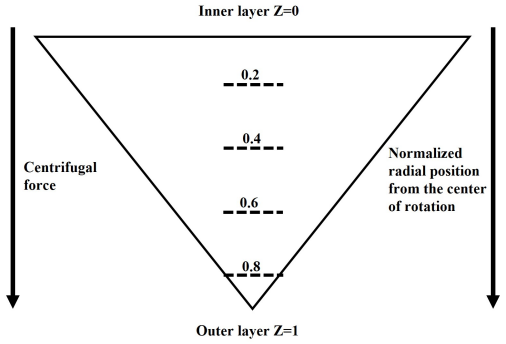

Figure 3. Schematics of the specimen.

We used an image analysis technique to post-process the SEM images, detect particle outlines, and measure the particle size distribution. An open-source image-processing software ImageJ [41] was utilized for this purpose. The images were divided into samples containing a minimum of 500 particles. The sample images were enhanced and binarized before the application of outline detection. The area of detected particles was then acquired and, finally, the equivalent area circle diameter x was calculated to be used afterward as a particle size. The areal fraction of a sample image occupied by the Al alloy particles was used to estimate the packing density. Due to the stochastic nature of the compaction process, statistical analysis was applied in our work, as it is considered as a valuable tool for studying segregation and mixing in powders [42,43]. This work used several different metrics to express the properties of the microstructure. The median diameter $x_m(Z)$ was chosen to represent the central tendency of the particle size distribution at position Z after centrifugal compaction. The initial median diameter of the powder $x_{m,0}$ before compaction was equal to 27 µm. To demonstrate the effect of centrifugal force, a difference in median particle size, Δx_m, was estimated as:

$$\Delta x_m = x_m(Z) - x_m(Z = 0). \quad (2)$$

The standard deviation of particle size from the median, σ_x, is given by:

$$\sigma_x^2 = \frac{1}{n-1} \sum_{i=1}^{n} (x_i - x_m)^2, \quad (3)$$

where n is the number of measured particles in a sample.

To describe the segregation process, this work employed a quasi-binary approach, which is commonly applied in multi-component powder analysis [42,43]. The quasi-binary approach was implemented by selecting a threshold diameter, in this case, the initial median $x_{m,0}$. Particles with size less than $x_{m,0}$ were considered as pseudo-component 1 with an initial concentration M_1, and particles with a size larger than $x_{m,0}$ as pseudo-component 2. The concentration of component 1 at different radial positions after centrifugal com-

paction was defined as M_{1j}. Using such an approach, we defined a segregation index, I_s as the characteristic of segregation:

$$I_s = \frac{\sigma_m}{M_1}, \tag{4}$$

where σ_m is the standard deviation of M_{1j} from M_1 at different sampling positions from the center of rotation of the centrifuge:

$$\sigma_m^2 = \frac{1}{k-1}\sum_{j=1}^{k}(M_{1j} - M_1)^2, \tag{5}$$

where k is the number of sampling positions (k = 4). Due to the threshold value being set to $x_{m,0}$, M_1 was equal to 0.5.

3. Results and Discussion

In the centrifugal field, the rate of separation in a suspension of particles mainly depends on the particle size and density. Particles of higher density or larger size travel at a faster rate and at some point they will be separated from the less dense or smaller particles. This phenomenon can be described according to the Stokes' law as [44,45]:

$$v = \frac{|\rho_{al} - \rho_m\,|GD_p^2\,g}{18\eta}, \tag{6}$$

where ρ_{al} is the Al particle density, ρ_m is the media density, D_p is the particle diameter and η is the viscosity coefficient of the media (high viscosity liquid-phase epoxy resin). Additionally, a number of studies were devoted to different factors that affect particle sedimentation during centrifugal process. For instance, Refs. [46–49] have been investigated the effect of side walls on the sedimentation velocity fluctuation. In [50], the authors studied a random particle clouds formation based on statistical mechanics. Li et al. [51] studied the sedimentation of particles in a high-viscosity liquid and confirmed that the sedimentation velocity increases with increasing particle volume fraction due to the formation of particle aggregates. Sum et al. [52] reviewed the effect of solution pH on coagulation behavior of nano and micro particles and found that the coagulation mechanisms differ significantly depending on pH and particle size. Additionally, attempts have been made to modify the Stokes model (Equation (6)) by taking into account the interactions of particles during sedimentation process and the wall effect [53,54]. Mityushev et al. [54] developed an advanced non-stationary sedimentation model of particles of different sizes and densities allowing for the time variation of the angular velocity and distance traveled by particle from the top of the vessel. The model was validated using experimental results on sedimentation of diamond-Ti_3 SiC_2 suspensions. The simulation results confirmed the possibility of formation of graded materials by centrifugal process due to particles segregation.

In our study, the moving direction of the particles in the centrifugal field is determined by the relative values of densities ρ_{al} and ρ_m: with Al powder density of 2.7 g/cm^3 , $\rho_{al} > \rho_m$, and particles move further away from the centrifugal center axis. Thus, Al particles will travel away from the centrifugal center axis under a centrifugal force according to Equation (6), and finally segregate in the outer layer of the spinning mold.

Figures 4–6 present the SEM images of the microstructure of samples obtained at different magnitudes of centrifugal forces. It should be noted that during the cutting and polishing processes, some particles detached, resulting in the formation of hollows. High compaction of powder is observed along the radial position for all values of centrifugal acceleration. Comparing the microstructure at different positions from the center of rotation, a similar trend may be noticed for all cases of centrifugal acceleration, which is coarsening of particles with radial position from the center of rotation. While this effect is not clearly visible for the case of compaction under G = 700 presented in Figure 4, other cases apparently indicate this trend. Comparing Figures 4–6, it can be stated that for high centrifugal forces (higher than G = 700) coarser Al particles are distributed in the outer

region, while the finer ones are in the inner region. This trend visibly indicates the segregation process, as the increase of the centrifugal force produces a greater separation of the particles, which are differentiated based on particle size. The segregation is especially conspicuous in Figure 6, where the mean particle size at $Z = 0.2$ is significantly smaller than at $Z = 0.8$.

The variation of the packing density of Al particles along the radial position of the green bodies is shown in Figure 7. As it can be seen, the packing density of the fabricated green bodies is high and in the range of 62 to 69%. The previous research works on the compaction of fine alumina particles with narrow size distribution using centrifugal forces resulted in the fabrication of green bodies with packing densities of 63% [14] and 63–68% [15]. These values of packing density were better than that of the sample (59%) compressed isostatically at 350 MPa [15].

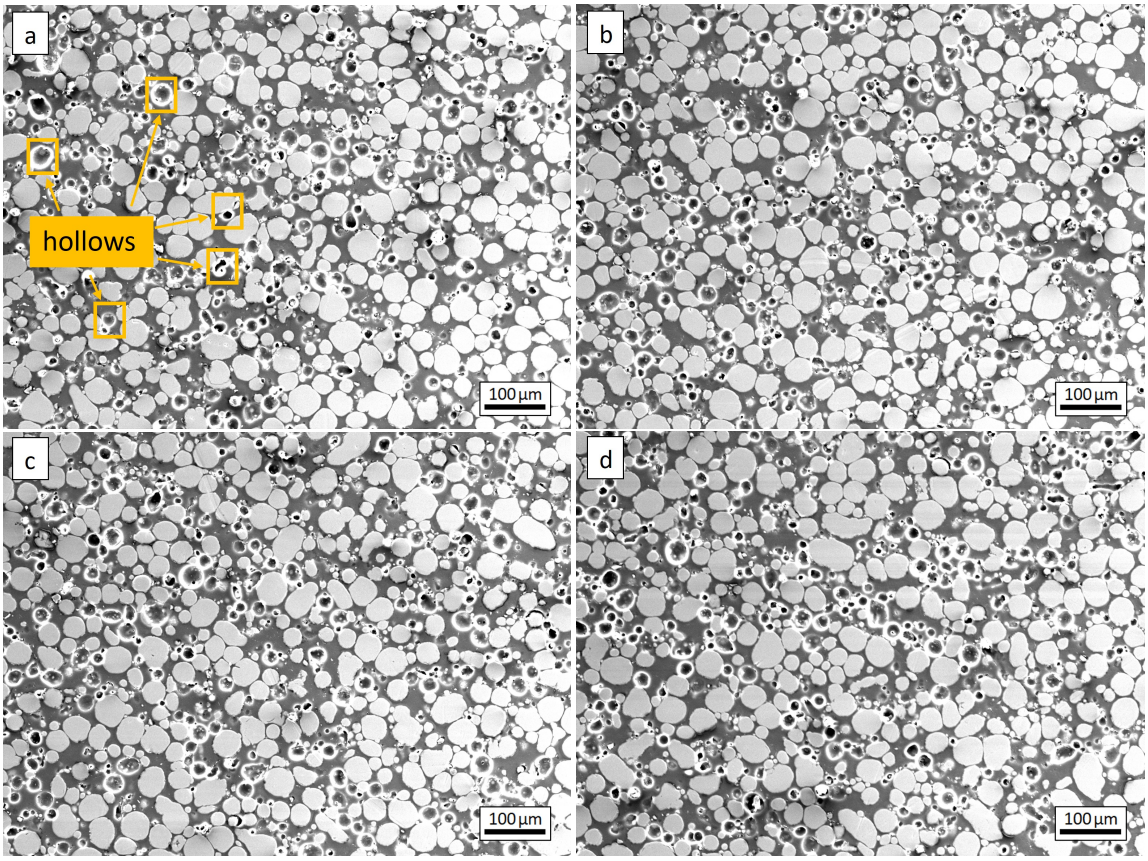

Figure 4. Microstructure of green body compacted under $G = 700$ at radial positions of (**a**) 0.2, (**b**) 0.4, (**c**) 0.6, and (**d**) 0.8.

Figure 7 shows that the packing density increases along the radial position for all values of centrifugal force. Consequently, the highest compaction is achieved at the outer layer and the lowest one at the inner layer. The highest packing density corresponds to the sample manufactured at $G = 3700$. However, it can be stated that no clear dependence of the packing density distribution on the centrifugal force is observed. This development can be explained by the long period of centrifugal casting. As shown in the study by Huisman et al. [15], the difference in centrifugal force mainly affects the velocity of sedimentation, but not the homogeneity of the compact density. Consequently, the same level of packing density can be achieved at lower G, but the time required for that is longer than at higher G. In the current study, all the specimens were under centrifugal force for 180 min each, which is shown to be a long enough time for the samples to reach approximately the same packing densities. In addition, the study by Huisman et al.

[15] concluded that there was no presence of plastic deformation of the specimen under the centrifugal force of G = 4000 after 15 min.

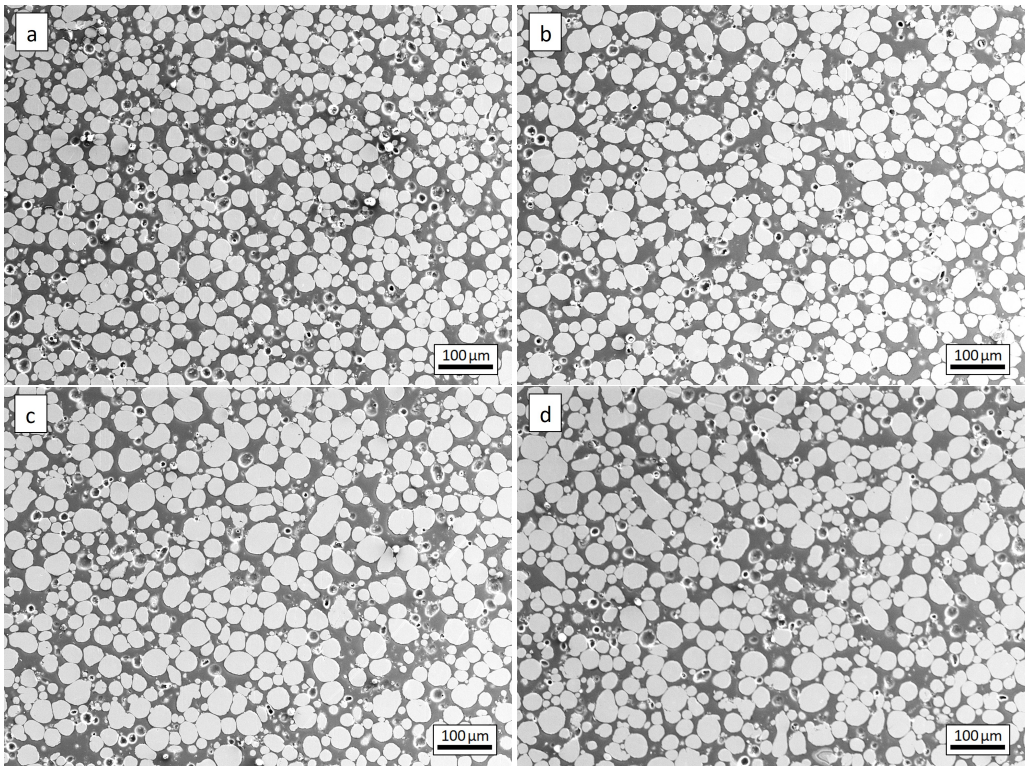

Figure 5. Microstructure of green body compacted under G = 1800 at radial positions of (**a**) 0.2, (**b**) 0.4, (**c**) 0.6, and (**d**) 0.8.

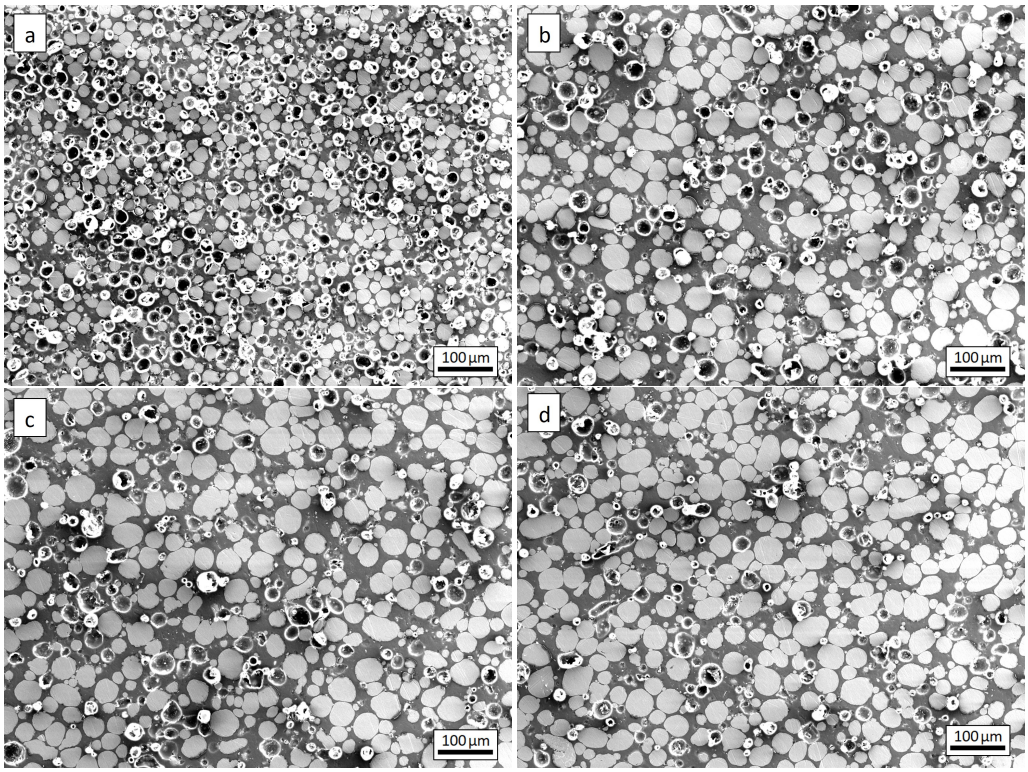

Figure 6. Microstructure of green body compacted under G = 3700 at radial positions of (**a**) 0.2, (**b**) 0.4, (**c**) 0.6, and (**d**) 0.8.

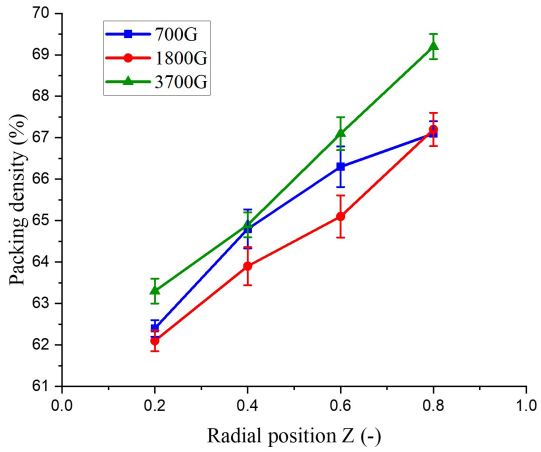

Figure 7. Radial distributions of packing density of green bodies prepared at various centrifugal forces.

Figure 8 shows the calculated values of Δx_m along with the radial position. For each case of centrifugal force, the median size increases with radial position, which means that finer particles were packed in the inner layer, while larger ones in the outer layer. In addition, it can be noticed that the difference in median diameters of the particles at the positions of 0.2 and 0.8 becomes more noticeable with the increase of centrifugal force. Such difference indicates that increasing centrifugal force results in higher segregation of Al particles.

Observing the standard deviation of the powder sizes presented in Figure 9, one can see a common trend: σ_x rapidly increases with radial position from $Z = 0.2$ to $Z = 0.4$, after which it remains approximately constant. A different trend is noticed in the case of $G = 700$. The value of σ_x correlates to the similarity between sizes of particles in a given sample, which means that the observed difference suggests the occurrence of segregation. Due to the wide distribution of the studied Al particles, there is a presence of both coarse and fine particles at positions further away from the center of rotation (outer layer), while positions closer to the center of rotation (inner layer) included more homogeneous distribution of smaller particles. Therefore, even though the positions of the particles under centrifugal force are graded according to the particles' size, finer particles still fit in the outer layer of the die. As seen in Figure 9, such segregation increases with centrifugal force, and at $G = 700$, the centrifugal compaction does not cause particles to segregate. As was mentioned before, this trend is observed in the SEM images presented in Figures 4–6.

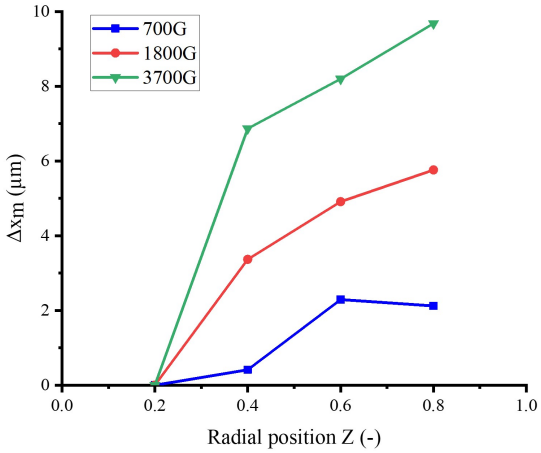

Figure 8. Difference in median particle diameter Δx_m versus radial position.

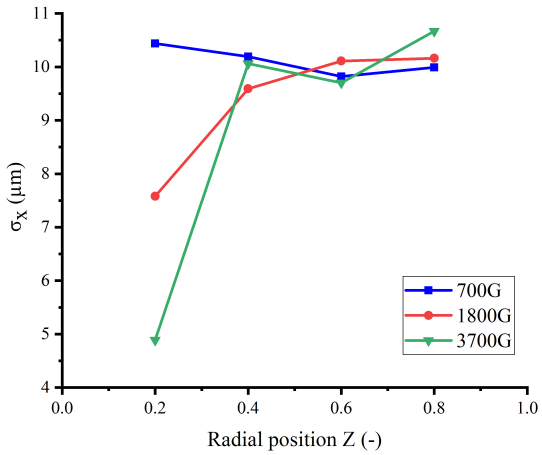

Figure 9. Standard deviation of equivalent particle diameters versus radial position.

Results presented in Figure 10 indicate that the values of σ_m are generally highest closer to the center of rotation and decrease further from the center, with an exemption of sample compacted at 700 G. The reasons for such trend are related to the high concentration of smaller particles, or pseudo-component 1, closer to the center, and approximately even distribution of both small and large particles at Z = 0.6 and Z = 0.8. These results denote the presence of both segregation and mixing effects: the particles are clearly separated according to their size, but both small and large pseudo-components are comparably present further from the center of rotation.

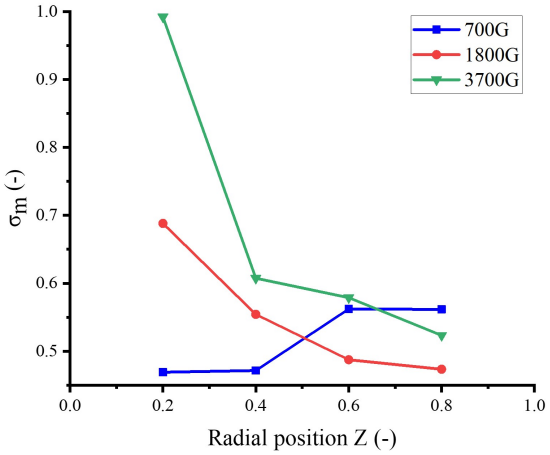

Figure 10. Standard deviation of particle concentrations versus radial position.

Figure 11 depicts the trend of the segregation index according to the centrifugal force. As expected, the segregation increases with increasing centrifugal force, and the sharpest transition occurs between 1800 G and 3700 G. To summarize, while the dependence between the magnitude of centrifugal force and the distribution of packing density over the radial position of the body was not clearly displayed, the results suggest the relation of the packing density on median particle size, as both increase further away from the center of rotation. A clear trend is also observed in the segregation phenomena. The separation of particles based on their size is observable both using of x_m and σ_x, and is especially explicit in the inner layer, between radial positions 0.2 and 0.4. Consequently, in the case of a high centrifugal force, using CCP on multi-sized powder results in the fabrication of FGM. The packing density is high across the radial position of samples, despite notable

segregation of the particles, which was observed in the pseudo-binary study of M_{1j}, σ_m, and I_s. Such effect was attributed to the wide distribution of particle sizes.

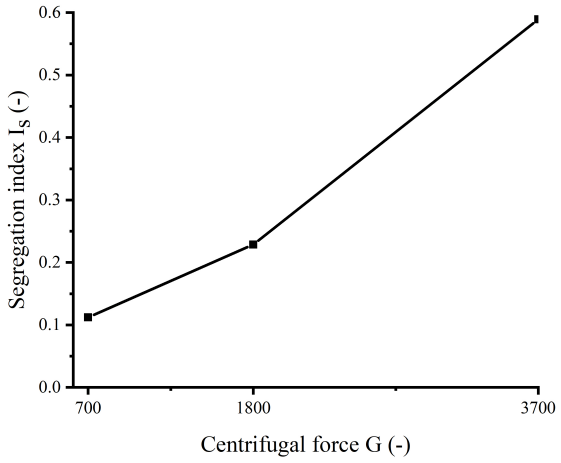

Figure 11. Variation of segregation index with centrifugal force.

4. Conclusions

This work studied the compaction of commercially available powder of Al alloy with multi-sized particles via centrifugal casting. The microstructure of the samples was observed at four different locations. The manufactured green bodies had excellent shape and high packing density. The results of the achieved level of compaction of the green samples with the multi-sized powder correspond with the studies made on fine powders with narrow particle size distribution. Therefore, the application of CCP on the multi-sized powder may be considered an effective compaction technique. In addition, the segregation effect of coarser and finer particles was observed. a study of the segregation index revealed that increasing centrifugal force results in higher segregation. Coarse particles pack in the outer layer of the green body and fine particles in the inner layer. However, the effect is not very explicit under the centrifugal force of $G = 700$. Overall, the study reveals that centrifugal casting is a promising way to manufacture highly compacted green bodies using not only fine powders with narrow particle size distribution, but multi-sized powders as well. Variation of the centrifugal force allows for controlling the segregation effect.

Author Contributions: Conceptualization, B.S. and A.A.; methodology, B.S.; software, D.A.; validation, B.S. and A.A.; formal analysis, B.S.; investigation, B.S.; resources, B.S.; data curation, B.S., A.A. and D.A.; writing—original draft preparation, B.S. and D.A.; writing—review and editing, B.S. and B.G.; visualization, B.S.; project administration, B.G. and C.S. All authors have read and agreed to the published version of the manuscript.

Funding: This research is funded by the Science Committee of the Ministry of Education and Science of the Republic of Kazakhstan (Grant No. AP09260422) and partially supported by the Nazarbayev University research grant (Grant No. OPCRP2020002).

Institutional Review Board Statement: Not applicable.

Informed Consent Statement: Not applicable.

Data Availability Statement: The data used in this research work can be made available upon request.

Conflicts of Interest: The authors declare no conflict of interest.

References

1. Torralba Castelló, J.M.; Campos Gómez, M. Toward high performance in Powder Metallurgy. *Rev. Metal.* **2014**, *50*, e017. [CrossRef]
2. Dondi, M. Powder Granulation and Compaction. In *Encyclopedia of Materials: Technical Ceramics and Glasses*; Pomeroy, M., Ed.; Elsevier: Oxford, UK, 2021; pp. 136–145. [CrossRef]

3. Bai, Y.; Li, L.; Fu, L.; Wang, Q. a review on high velocity compaction mechanism of powder metallurgy. *Sci. Prog.* **2021**, *104*, 00368504211016945. [CrossRef] [PubMed]
4. Verhaeghe, B.; Courtois, C.; Petit, F.; Cambier, F.; Guérin, J.D.; Leriche, A.; Hampshire, S. Lighter tableware ceramic by controlling porosity: Effect of porosity on mechanical properties. *Ceram. Int.* **2014**, *40*, 763–770. [CrossRef]
5. Law, M.; Hulme-Smith, C.N.; Matsushita, T.; Jönsson, P.G. Assessment of mechanisms for particle migration in semi-solid high pressure die cast aluminium-silicon alloys. *J. Manuf. Mater. Process.* **2020**, *4*, 51. [CrossRef]
6. Gain, A.K.; Song, H.Y.; Lee, B.T. Microstructure and mechanical properties of porous yttria stabilized zirconia ceramic using poly methyl methacrylate powder. *Scr. Mater.* **2006**, *54*, 2081–2085. [CrossRef]
7. Suzuki, M.; Oshima, T. Verification of a model for estimating the void fraction in a three-component randomly packed bed. *Powder Technol.* **1985**, *43*, 147–153. [CrossRef]
8. Thirupathi, N.; Kumar, R.; Kore, S.D. Experimental and numerical investigations on electromagnetic powder compaction of Aluminium 6061 alloy powder. *Powder Technol.* **2022**, *406*, 117579. [CrossRef]
9. Abdizadeh, H.; Ebrahimifard, R.; Baghchesara, M.A. Investigation of microstructure and mechanical properties of nano MgO reinforced Al composites manufactured by stir casting and powder metallurgy methods: a comparative study. *Compos. Part B Eng.* **2014**, *56*, 217–221. [CrossRef]
10. Westman, A.R.; Hugill, H. the packing of particles 1. *J. Am. Ceram. Soc.* **1930**, *13*, 767–779. [CrossRef]
11. McGeary, R. Mechanical packing of spherical particles. *J. Am. Ceram. Soc.* **1961**, *44*, 513–522. [CrossRef]
12. Taskiran, M.; Demirkol, N.; Capoglu, A. Influence of mixing/milling on sintering and technological properties of anorthite based porcelainised stoneware. *Ceram. Int.* **2006**, *32*, 325–330. [CrossRef]
13. Lieberman, M.A.; Lichtenberg, A.J. *Principles of Plasma Discharges and Materials Processing*; John Wiley & Sons: Hoboken, NJ, USA, 2005.
14. Suzuki, H.Y.; Kuroki, H. Development of High-Speed Centrifugal Compaction Process of Alumina. *Adv. Sci. Technol. Trans. Technol. Publ.* **2006**, *45*, 421–426.
15. Huisman, W.; Graule, T.; Gauckler, L. Alumina of high reliability by centrifugal casting. *J. Eur. Ceram. Soc.* **1995**, *15*, 811–821. [CrossRef]
16. Porter, Q.; Li, X.; Ma, C. Pressing and Infiltration of Metal Matrix Nanocomposites. *J. Manuf. Mater. Process.* **2021**, *5*, 54. [CrossRef]
17. Gao, J.; Wang, C. Modeling the solidification of functionally graded materials by centrifugal casting. *Mater. Sci. Eng. A* **2000**, *292*, 207–215. [CrossRef]
18. Watanabe, Y.; Yamanaka, N.; Fukui, Y. Control of composition gradient in a metal-ceramic functionally graded material manufactured by the centrifugal method. *Compos. Part a Appl. Sci. Manuf.* **1998**, *29*, 595–601. [CrossRef]
19. Liu, D.M.; Lin, J.T. Influence of ceramic powders of different characteristics on particle packing structure and sintering behaviour. *J. Mater. Sci.* **1999**, *34*, 1959–1972. [CrossRef]
20. Chang, J.C.; Velamakanni, B.V.; Lange, F.F.; Pearson, D.S. Centrifugal consolidation of Al_2O_3 and AI_2O_3/ZrO_2 composite slurries vs interparticle potentials: Particle packing and mass segregation. *J. Am. Ceram. Soc.* **1991**, *74*, 2201–2204. [CrossRef]
21. Janković Ilić, D.; Fiscina, J.; Oliver, C.G.; Ilić, N.; Mücklich, F. Self Formed Cu-W Functionally Graded Material Produced Via Powder Segregation. *Adv. Eng. Mater.* **2007**, *9*, 542–546. [CrossRef]
22. Chmielewski, M.; Pietrzak, K. Metal-ceramic functionally graded materials–manufacturing, characterization, application. *Bull. Pol. Acad. Sci. Tech. Sci.* **2016**, *64*, 151–160. [CrossRef]
23. Cannillo, V.; Lusvarghi, L.; Manfredini, T.; Montorsi, M.; Siligardi, C.; Sola, A. Glass–ceramic functionally graded materials produced with different methods. *J. Eur. Ceram. Soc.* **2007**, *27*, 1293–1298. [CrossRef]
24. Besisa, D.H.; Ewais, E.M. Advances in functionally graded ceramics—Processing, sintering properties and applications. *Adv. Funct. Graded Mater. Struct.* **2016**, 1–32. DOI: 10.5772/62612. [CrossRef]
25. Hasanov, S.; Alkunte, S.; Rajeshirke, M.; Gupta, A.; Huseynov, O.; Fidan, I.; Alifui-Segbaya, F.; Rennie, A. Review on additive manufacturing of multi-material parts: Progress and challenges. *J. Manuf. Mater. Process.* **2021**, *6*, 4. [CrossRef]
26. Tripathy, A.; Sarangi, S.K.; Panda, R. Fabrication of functionally graded composite material using powder metallurgy route: an overview. *Int. J. Mech. Prod. Eng. Res. Dev.* **2017**, *7*, 135–146.
27. Fukui, Y. Fundamental investigation of functionally gradient material manufacturing system using centrifugal force. *JSME Int. J. Ser. 3 Vib. Control. Eng. Eng. Ind.* **1991**, *34*, 144–148. [CrossRef]
28. Chirita, G.; Soares, D.; Silva, F. Advantages of the centrifugal casting technique for the production of structural components with Al–Si alloys. *Mater. Des.* **2008**, *29*, 20–27. [CrossRef]
29. Jamian, S.; Watanabe, Y.; Sato, H. Formation of compositional gradient in Al/SiC FGMs fabricated under huge centrifugal forces using solid-particle and mixed-powder methods. *Ceram. Int.* **2019**, *45*, 9444–9453. [CrossRef]
30. Watanabe, Y.; Inaguma, Y.; Sato, H.; Miura-Fujiwara, E. a novel fabrication method for functionally graded materials under centrifugal force: the centrifugal mixed-powder method. *Materials* **2009**, *2*, 2510–2525. [CrossRef]
31. Sato, H.; Maeda, J.; Yamada, M.; Watanabe, Y. Effects of Particle Size on Fabrication of Al-TiO_2 Functionally Graded Materials by Centrifugal Mixed-Powder Method. *Mater. Sci. Forum. Trans. Technol. Publ.* **2017**, *879*, 1691–1697. [CrossRef]
32. Sato, H.; Inaguma, Y.; Watanabe, Y. Fabrication of Cu-based functionally graded materials dispersing fine SiC particles by a centrifugal mixed-powder method. *Mater. Sci. Forum. Trans. Technol. Publ.* **2010**, *638*, 2160–2165. [CrossRef]

33. Watanabe, Y.; Miura-Fujiwara, E.; Sato, H.; Takekoshi, K.; Tsuge, H.; Kaga, T.; Bando, N.; Yamagami, S.; Kurachi, K.; Yokoyama, H. Fabrication of functionally graded grinding wheel by a centrifugal mixed-powder method for CFRP-drilling applications. *Int. J. Mater. Prod. Technol.* **2011**, *42*, 29–45. [CrossRef]
34. Shinohara, K.; Golman, B. Segregation indices of multi-sized particle mixtures during the filling of a two-dimensional hopper. *Adv. Powder Technol.* **2002**, *13*, 93–107. [CrossRef]
35. Chung, Y.C.; Liao, C.C.; Zhuang, Z.H. Experimental investigations for the effect of fine powders on size-induced segregation in binary granular mixtures. *Powder Technol.* **2021**, *387*, 270–276. [CrossRef]
36. Kondoh, K.; Watanabe, R.; Hashimoto, H. Analysis of compaction behaviour of wet granulated aluminium alloy powder. *Powder Metall.* **2000**, *43*, 359–363. [CrossRef]
37. Sohn, H.Y.; Moreland, C. the effect of particle size distribution on packing density. *Can. J. Chem. Eng.* **1968**, *46*, 162–167. [CrossRef]
38. Desmond, K.W.; Weeks, E.R Influence of particle size distribution on random close packing of spheres. *Phys. Rev. E* **2014**, *90*, 022204. [CrossRef]
39. Young, Z.; Qu, M.; Coday, M.M.; Guo, Q.; Hojjatzadeh, S.M.H.; Escano, L.I.; Fezzaa, K.; Chen, L. Effects of Particle Size Distribution with Efficient Packing on Powder Flowability and Selective Laser Melting Process. *Materials* **2022**, *15*, 705. [CrossRef]
40. Watanabe, Y.; Kawamoto, A.; Matsuda, K. Particle size distributions in functionally graded materials fabricated by the centrifugal solid-particle method. *Compos. Sci. Technol.* **2002**, *62*, 881–888. [CrossRef]
41. Rasband, W.S. Imagej, Us National Institutes of Health, Bethesda, Maryland, USA. 2011. Available online: http://imagej.nih.gov/ij/ (accessed on 12 June 2022).
42. Fan, L.; Too, J.; Rubison, R.; Lai, F. Studies on multicomponent solids mixing and mixtures Part III. Mixing indices. *Powder Technol.* **1979**, *24*, 73–89. [CrossRef]
43. Shinohara, K.; Golman, B.; Nakata, T. Size segregation of multicomponent particles during the filling of a hopper. *Adv. Powder Technol.* **2001**, *12*, 33–43. [CrossRef]
44. Ogawa, T.; Watanabe, Y.; Sato, H.; Kim, I.S.; Fukui, Y. Theoretical study on fabrication of functionally graded material with density gradient by a centrifugal solidparticle method. *Compos. Part a Appl. Sci. Manuf.* **2006**, *37*, 2194–2200. [CrossRef]
45. Lin, X.; Liu, C.; Xiao, H. Fabrication of Al–Si–Mg functionally graded materials tube reinforced with in situ Si/Mg2Si particles by centrifugal casting. *Compos. Part B Eng.* **2013**, *45*, 8–21. [CrossRef]
46. Brenner, M.P. Screening mechanisms in sedimentation. *Phys. Fluids* **1999**, *11*, 754–772. [CrossRef]
47. Ladd, A. Effects of container walls on the velocity fluctuations of sedimenting spheres. *Phys. Rev. Lett.* **2002**, *88*, 048301. [CrossRef] [PubMed]
48. Nicolai, H.; Peysson, Y.; Guazzelli, É. Velocity fluctuations of a heavy sphere falling through a sedimenting suspension. *Phys. Fluids* **1996**, *8*, 855–862. [CrossRef]
49. Guazzelli, E. Evolution of particle-velocity correlations in sedimentation. *Phys. Fluids* **2001**, *13*, 1537–1540. [CrossRef]
50. Ekiel-Jeżewska, M.; Metzger, B.; Guazzelli, E. Spherical cloud of point particles falling in a viscous fluid. *Phys. Fluids* **2006**, *18*, 038104. [CrossRef]
51. Li, C.; Zhou, P.; Yan, Y.; Luo, X.; He, T.; Wang, X. Influence of inelastic collision on the dynamic behavior of particle sedimentation in high-viscosity fluids. *Adv. Powder Technol.* **2022**, *33*, 103673. [CrossRef]
52. Sun, H.; Jiao, R.; Xu, H.; An, G.; Wang, D. the influence of particle size and concentration combined with pH on coagulation mechanisms. *J. Environ. Sci.* **2019**, *82*, 39–46. [CrossRef]
53. Jones, R.; Kutteh, R. Sedimentation of colloidal particles near a wall: Stokesian dynamics simulations. *Phys. Chem. Chem. Phys.* **1999**, *1*, 2131–2139. [CrossRef]
54. Mityushev, V.; Jaworska, L.; Rozmus, M.; Królicka, B. Compaction of the diamond–Ti_3SiC_2 graded material by the high–speed centrifugal compaction process. *Arch. Mater. Sci. Eng.* **2007**, *28*, 677–682.